TISSUE ENGINEERING: Part C
Volume 24, Number 1, 2018

DOI: 10.1089/ten.tec.2017.0236

termis
Tissue Engineering
& Regenerative Medicine
International Society

METHODS ARTICLE

Noninvasive Absolute Electron Paramagnetic Resonance Oxygen Imaging for the Assessment of Tissue Graft Oxygenation

Mrignayani Kotecha, PhD,[1] Boris Epel, PhD,[2] Sriram Ravindran, PhD,[3] Deborah Dorcemus, BS,[4] Syam Nukavarapu, PhD,[4] and Howard Halpern, MD, PhD[2]

Oxygen is the single most important molecule for sustaining life and, therefore, an important variable in tissue engineering and regenerative medicine. It has been shown that the change in oxygen concentration in an artificial or tissue-engineered graft affects cell survival, differentiation, and tissue growth in profound ways. However, at present, there are no reliable methods to map partial oxygen pressure (pO_2) in growing artificial tissues. Here, we adapt and test the suitability of electron paramagnetic resonance oxygen imaging (EPROI) in assessing tissue graft oxygenation *in vitro*. EPROI is an established method to assess absolute pO_2 and has been widely applied to study tumor hypoxia in small animals. In this study, we demonstrate the feasibility of EPROI in evaluating oxygen dynamics in tissue grafts. We measured oxygen concentration in mesenchymal stem cell (MSC)-seeded polylactic-*co*-glycolic acid (PLGA) scaffolds with variable porosity. The pO_2 maps of these scaffolds showed that the mean pO_2 inside the scaffolds was smaller than the ambient air pO_2 (21% oxygen, 160 torr) and was gradually increased with increasing pore size. We assessed the local oxygen dynamics of the MSC-seeded osteogenic scaffold made from collagen–chitosan hydrogels in a partially sealed Eppendorf tube. The change in pO_2 values as a function of time inside the graft showed that the cells had used available oxygen within first 2 h of the experiment and then went to a dormant low oxygen consumption state until the oxygen supply was reestablished. Collectively, these data suggest that EPROI could be successfully used for mapping pO_2 in tissue-engineered grafts. The knowledge of tissue graft oxygenation may be used to improve scaffold design and to assess the tissue viability and growth.

Keywords: 3D oxygen imaging, tissue graft assessment, electron paramagnetic resonance oxygen imaging

Introduction

Tissue engineering and regenerative medicine (TERM) has the immense therapeutic potential to treat a wide range of medical conditions from orthopedic injuries to the liver and cardiovascular diseases, traumatic brain injuries, diabetes, etc.[1–5] TERM combines biocompatible scaffolds with appropriate cells and devises cell growth conditions to create an engineered graft that can replace or repair damaged tissue.[6]

Oxygen is an important vital molecule to sustain aerobic life forms. It has been shown that oxygen deficiency at the center of three-dimensional (3D) tissue-engineered grafts can cause cell necrosis.[7] It has also been shown that stem cell differentiation can be influenced by controlling oxygen pressure.[8–10] Higher oxygen consumption rate was shown to lead to better islet performances in the bioartificial pancreas.[11,12] Therefore, for the success of TERM, methods for noninvasive assessment of partial oxygen pressure (pO_2) in tissues are of paramount importance.[13]

Currently, there is no reliable method available to scientists for mapping pO_2 noninvasively. Commonly, the oxygen tension in engineered tissues is measured using pulse oximetry, electrodes, or oxygen-quenched luminescence.[14,15] These

[1]O2M Technologies, LLC, Chicago, Illinois.
[2]Department of Radiation and Cellular Oncology, Center for EPR Imaging In Vivo Physiology, The University of Chicago, Chicago, Illinois.
[3]Department of Oral Biology, College of Dentistry, University of Illinois at Chicago, Chicago, Illinois.
[4]Orthopaedic Surgery and Department of Biomedical Engineering, University of Connecticut, Farmington, Connecticut.

methods provide oxygen measurement at a single point or average pO_2 over the volume. Some of the methods are invasive and are not suitable for repetitive or *in vivo* oxygen measurements. Optical methods have restricted penetration depth of few millimeters. Magnetic resonance imaging (MRI)-based methods such as ^{19}F MRI are less precise but suitable for measurements deep in tissues. However, the insoluble ^{19}F probes have to be injected directly to the place of measurement. ^{17}O MRI suffers from the low signal-to-noise ratio and the prohibitive cost of ^{17}O molecular probes. Recent literature shows that the efforts are underway to improve the specificity and suitability of ^{19}F and ^{17}O MRI techniques for oxygen assessment in tissue-engineered grafts.[16,17]

Electron paramagnetic resonance oxygen imaging (EPROI) is an established noninvasive absolute oxygen mapping technique based on principles similar to MRI.[18,19] EPR detects unpaired electron spins subjected to the constant uniform magnetic field by manipulating them using radio frequency electromagnetic radiation. Similar to MRI, EPROI uses magnetic field gradients to generate spatial images.[18] In contrast to 1.5 T MRI, 250 MHz EPROI relies on 166 times smaller magnetic field (9 mT) generated by the cryogen-free magnet and magnetic field gradients that do not change during signal detection.[20] EPROI measures the relaxation maps of a water-soluble oxygen-reporting trityl molecule that distributes in a body upon injection[21–25] and converts them into oxygen images.

Over the past decade, EPROI has advanced at a rapid pace to deliver 1–10 min oxygen images in live mice, rats, and rabbit limbs with oxygen resolution and absolute accuracy of 1 torr and spatial resolution 1 mm.[21] For oxygen sensing, we used water soluble deuterated OX063 trityl spin probe.[20] The EPROI has been found to be well correlated with Oxylite probe *in vivo*.[24] The EPROI has been widely used for mapping tumor hypoxia for evaluating oxygenation-related tumor drug efficiency and, recently, for improving radiation efficiency.[19,20,25] However, its use for mapping pO_2 of tissue-engineered grafts is only starting to get consideration.[26] In this study, we test the feasibility of EPROI for assessing tissue graft oxygenation *in vitro* for two commonly used biomaterials in TERM. Two different models of tissue grafts were used in this study. In the first experiment, the osteogenic tissue grafts were made of mesenchymal stem cell (MSC)-seeded poly(lactide-*co*-glycolide) (PLGA) microbeads with varying porosity. In this material, our aim was to correlate pO_2 maps with cell survival data published in our previous work.[7,27,28] The second osteogenic tissue grafts were made using human marrow stromal cell-seeded collagen–chitosan hydrogel scaffolds. The hydrogel-based grafts are known for excellent oxygen transport properties *in vitro*. Here, our aims were to demonstrate the feasibility of acquiring local oxygen dynamics in response to an external change of pO_2 and assess the cell viability using EPROI.

Materials and Methods

Optimization of oxygen imaging experiments

All EPROI experiments were performed using the 250 MHz pulse EPR imager with a 19 mm resonator constructed at the University of Chicago (Fig. 1A).[23] Using cell-seeded fully oxygenated 1 mg/mL collagen gel, we optimized OX063 concentration in the gel necessary for pO_2 measurements (Fig. 1B). Figure 2 shows that 1 mM concentration is suitable for our measurements and the spin probe is equally distributed within the sample. We also found that uniform distribution of OX063 spin probe in the sample requires about 30 min after the introduction of the spin probe to the sample.

PLGA scaffolds with varying porosity and pO_2 measurements

Poly (85 lactide-*co*-15 glycolide, PLGA 85:15; Evonik, Germany) was dissolved in methylene chloride and fabricated into microspheres using an oil-in-water emulsion procedure. Microspheres, with a size range of 425–600 μm, were collected and mixed with 0, 20, or 40 weight percentage NaCl porogen (size range 200–300 μm).[29] The combinations were placed in a 5 mm diameter × 10 mm height scaffold mold and were allowed to be thermally sintered at 100°C for 1 h. Porogen leaching with water was used to create low porous (0% NaCl), medium porous (20% NaCl), and highly porous scaffolds (40% NaCl). As published earlier, the low-porosity

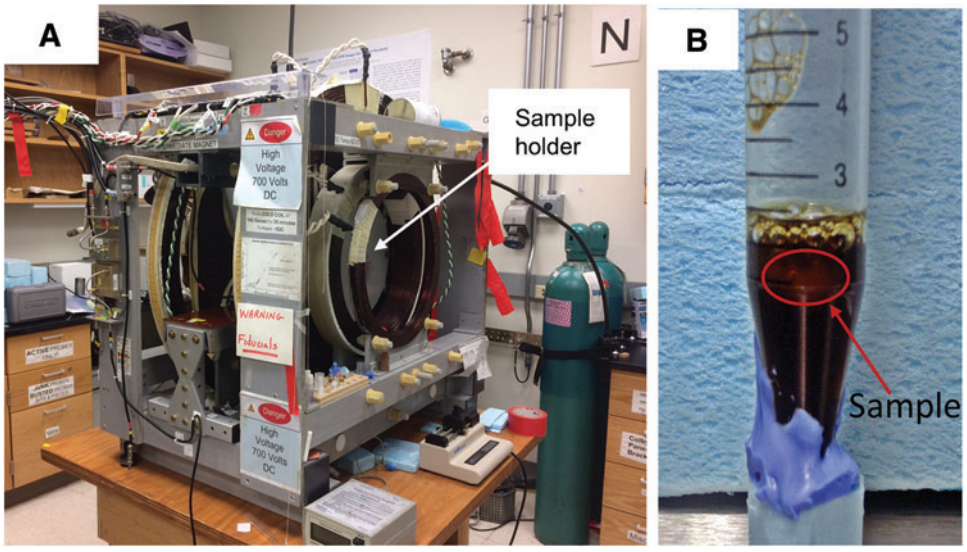

FIG. 1. **(A)** EPR oxygen imaging instrument setup at the University of Chicago, **(B)** stem cells (250K)-seeded collagen gel with 1 mM OX063 spin probe in an Eppendorf tube, the sample boundary is drawn with *red*. The gel sample was residing on *top* of the medium and equilibrated with ambient oxygen (21%) at all time. EPR, electron paramagnetic resonance. Color images available online at www.liebertpub.com/tec

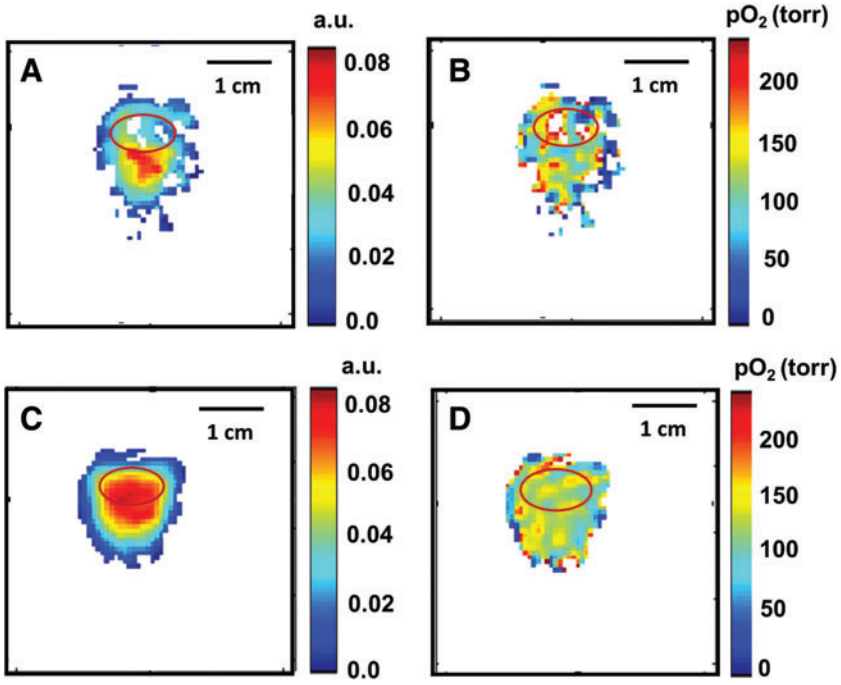

FIG. 2. Distribution of OX063 in collagen gel sample for 0.5 mM concentration **(A)** and 1 mM concentration **(C)** and pO_2 maps for 0.5 mM **(B)** and 1 mM **(D)** OX063 concentration. The mean pO_2 in 1 mM concentration was 128 ± 2.4 torr, showing excellent oxygen diffusion capability of collagen hydrogel. pO_2, partial oxygen pressure. Color images available online at www.liebertpub.com/tec

graft has most pores in the range of 100–300 μm, whereas the medium and highly porous scaffolds have increasingly larger pores (300–500 μm).[27]

Bone marrow-derived human mesenchymal stem cells (hMSCs) were isolated using Magellan® and MACS® technologies and cultured in regular basal medium (DMEM/F-12 + GlutaMAX, with 10% fetal bovine serum and 1% P/S) at 5% CO_2 and 87% humidity.[30] Cells were frozen after third passage and used at fifth passage. Low, medium, and highly porous scaffolds were sterilized in 70% ethanol solution (15 min) followed by ultraviolet treatment for 15 min on each side. Once sterilized, fifth passage hMSCs were extracted and 250,000 cells were seeded onto the top end of each scaffold. The cells were allowed to attach to the matrix for 1 h before the addition of medium. The constructs were cultured for 14 days in basal medium, medium was changed every 2–3 days. The EPROI experiments were performed at day 15.

The PLGA constructs with 1 mM OX063 dissolved in growth medium were placed in a 1.5 mL Eppendorf tube (Fig. 3A). The tubes were open to ambient air throughout the experiments. A series of 20 min long spin-lattice relaxation-based pO_2 images were acquired.

Collagen–chitosan-based osteogenic graft and pO_2 measurements

The graft material was created by seeding 1 million human marrow stromal cells in collagen–chitosan (1:1 mg/mL) hydrogel. The tissue was cultured for 14 days in mineralization medium with 5% CO_2, and the medium was changed every 2–3 days. The EPROI experiments were performed at day 15. We have previously shown excellent osteogenic properties of these tissue grafts.[31,32] An acellular tissue graft was also prepared to be used as a control in oxygen dynamics experiments.

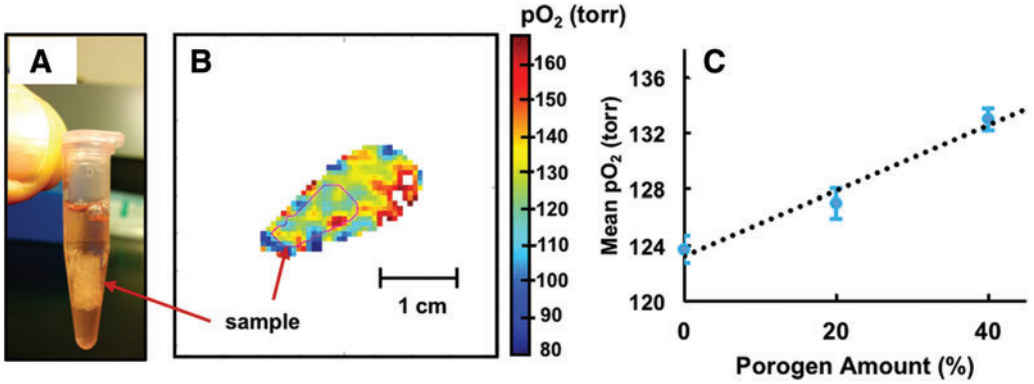

FIG. 3. **(A)** A representative PLGA scaffold in an Eppendorf tube, **(B)** an example of pO_2 map of PLGA scaffold. A slice showing pO_2 map of the sample **(C)** mean pO_2 as a function of porogen percentage ($n = 1$). The *dashed line* represents the trend. The *bars* represent standard errors. The mean pO_2 increased with the increase in porosity. PLGA, polylactide-*co*-glycolide. Color images available online at www.liebertpub.com/tec

The tissue graft sample was placed in a 1.5 mL Eppendorf tube and 1 mM OX063 dissolved in medium was filled to the top of the tube to limit the available oxygen to the sample and the tube was closed and sealed. A series of 20 min long spin-lattice relaxation-based pO_2 images were taken every 20 min. After 7 h of the experiment, the tube was opened and another hour of imaging was performed. For control, the sealed tube was measured for 4 h, and when no change in pO_2 values was found, the experiment was stopped.

Results and Discussion

Figure 1A shows the 250 MHz EPR imaging instrument used in this study. To test the accessibility of spin probe OX063 to common biomaterials used in tissue engineering applications, we used a sample with MSCs-seeded (250,000/scaffold) collagen gel (1 mL/mg). The OX063 was added to the sample medium as shown in Figure 1B. The final concentration of OX063 in the sample was optimized to obtain reasonable signal-to-noise ratio for fully oxygenated samples. The intensity of the OX063 signal is strongly dependent on oxygen concentration and drops nearly three times when pO_2 changes from 0% to 21%. For the imaging of low pO_2, a concentration of 0.3 mM is typically sufficient; however, at ambient air experiments, 1 mM concentration is found to be suitable for experiments. Figure 2 shows the distribution of OX063 within the sample and the surrounding medium. Inversion recovery spin-lattice relaxation-based pO_2 imaging was performed. The oxygen image shown in Figure 2B and D is inferred from the linear relationship between the relaxation rate of OX063 and the oxygen concentration as published previously.[20] The intensity of EPR signal was found to be similar in the medium and in the sample because of excellent oxygen diffusion characteristics of hydrogels. The average pO_2 in this sample was 128 ± 2.4 torr. The pO_2 in the tube is smaller than the ambient air (21% oxygen, $pO_2 = 160$ torr at 1 atmospheric pressure at 20°C temperature). It has been known that the dissolved oxygen pressure in culture medium is smaller (18%, 136.8 torr) than the ambient air because of other factors such as temperature and salinity of medium that affect the oxygen solubility in the medium.[33] The pO_2 values obtained by EPROI are in close agreement with these observations.

Figure 3 shows PLGA scaffolds (Fig. 3A) with an example pO_2 map (Fig. 3B). The approximate sample boundary from computed tomography (CT) images is drawn in red. One of the coauthors previously established the role of scaffold pore volume in the matrix pO_2. In this study, several PLGA grafts with controlled pore size and volume were fabricated, which were referred to oxygen-tension controlled matrices. The study directly measured engineered scaffold local pO_2 using a needle-type fiber optic microsensor and correlated oxygen tension measurements with the scaffold pore sizes. The measurements, as well as the cell survival studies, reveal that the matrices with the high amount of large size pores (300–500 μm) show increased oxygen tension.[7,27]

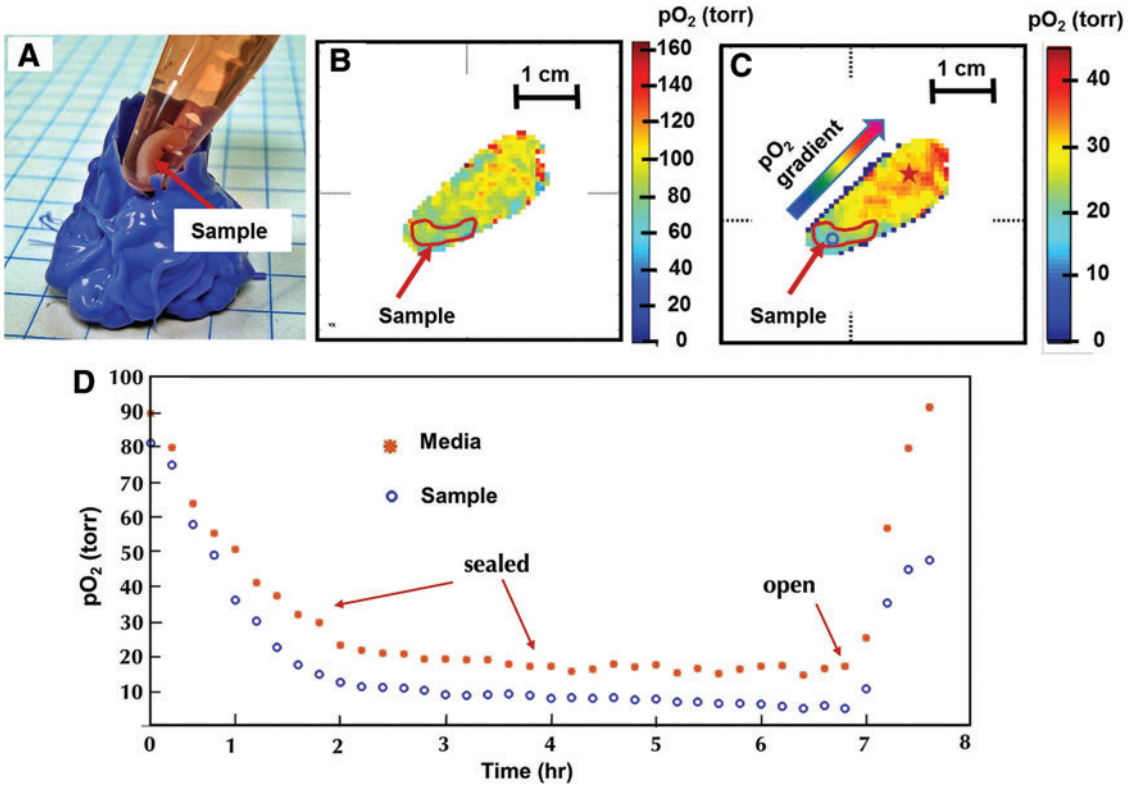

FIG. 4. **(A)** Osteogenic tissue graft in a 1.5 mL Eppendorf tube with medium, **(B)** pO_2 map of sample with medium after the tube was partially sealed. **(C)** pO_2 map after ~2 h after first measurement, pO_2 gradient is visible in the sample as well as in the tube as cells are consuming available oxygen, **(D)** pO_2 dynamics for voxels inside the sample (denoted by a *blue circle* in **C**) and adjacent medium (denoted by a *red star* in **C**) as a function of time. The measurement was done with the closed tube for 7 h and then another 1 h after opening the tube. Color images available online at www.liebertpub.com/tec

In this study, the mean pO_2 values inside the grafts were 123.7 ± 1.0, 127.0 ± 1.1, and 133.0 ± 0.8 torr, for 0%, 20%, and 40% NaCl samples, respectively. Figure 3C shows the graphical representation of change in mean pO_2 values as a function of porogen percentage. The mean pO_2 for adjacent medium in 5 voxel radius was 142.06 ± 0.5 torr. The pO_2 values in all samples were found to be lower than in the adjacent medium, which corroborates earlier studies.[7,27] This example illustrates the usefulness of oxygen imaging for 3D porous scaffolds. As explained earlier, a major bottleneck in using 3D porous scaffold is the lack of oxygen and nutrients deep inside the growing tissue that causes cell necrosis. The availability of noninvasive oxygen imaging technique may help improve scaffold design and may potentially be useful for many applications such as large area bone regeneration.

Figure 4A shows cell-seeded collagen–chitosan-based osteogenic tissue graft in an Eppendorf tube. In pO_2 maps (Fig. 3B, C), the sample at the bottom of the tube with low oxygen concentration and the culture medium on top of the sample is clearly distinguishable. The approximate sample boundary from CT images is drawn in red. Figure 4B shows the first pO_2 image ~ 30 min after the tube was sealed. The cells start consuming oxygen quickly, and the pO_2 gradient between medium and scaffold becomes clearly visible after ~ 2 h of measurement. After about 2 h, cells stay in a hypoxic mode with little change in pO_2. After the tube had been opened, the oxygen pressure returned quickly to normal. The change in local oxygen pressure as a function of time within the sample and the medium is shown in Figure 4D. The calculated oxygen consumption rate (OCR) was 0.74 torr/min during the active state (first hour) and 0.0046 torr/min during the dormant state (fourth hour) of cells at the site of voxel depicted with a blue circle in Figure 3C. This example illustrates the utility of oxygen imaging to probe local oxygen consumption rate. It may also be used to control stem cell differentiation by modulating oxygen pressure as desired.

Conclusions

In this study, we show the feasibility of *in vitro* EPROI in assessing oxygenation and cell dynamics in tissue grafts made from common biomaterials. The EPROI provides 3D maps of tissue oxygenation noninvasively. These studies show that EPROI is a robust technology that can be utilized in conjunction with the standard assessment. The 3D oxygen maps may potentially be translated into assessing cell viability, modulating oxygen pressure for optimizing stem cell differentiation, or enhancing designs of cell entrapment devices and scaffolds. Further work is underway to adapt the technique to different tissue grafts models, and when established, the EPROI may become an invaluable tool in TERM. In the future, we plan to extend our study to *the* assessment of tissue grafts in animals.

Acknowledgments

Dr. Nukavarapu acknowledges funding from AO Foundation S-13-122N, Musculoskeletal Transplant Foundation, National Science Foundation (EFRI-REM, EFMA) 1640008, and Connecticut Innovations Biopipeline Program. B.E. and H.H. acknowledge the support from NIH P41 EB002034. B.E. acknowledges R50 CA 211408. Dr. Ravindran acknowledges funding from NIH grant DE 023806. M.K. acknowledges NSF I-Corp 1347383 grant.

Disclosure Statement

No competing financial interests exist. Dr. Kotecha, Dr. Epel and Dr. Halpern are owners of O2M Technologies, LLC that is developing a high field preclinical oxygen imager (25 mT, 720 MHz) for tissue graft assessment.

References

1. Vacanti, J., and Vacanti, C.A. Chapter One—The History and Scope of Tissue Engineering. Principles of Tissue Engineering, 3rd ed. Burlington: Academic Press, 2007, p. 3.
2. Langer, R., and Vacanti, J. Tissue engineering. Science **260,** 920, 1993.
3. Chen, B., Liebman, C., Rabbani, P., and Cho, M. Stem Cell Tissue Engineering and Regenerative Medicine. Magnetic Resonance Imaging in Tissue Engineering. Hoboken, NJ: John Wiley & Sons, Inc., 2017, p. 1.
4. Fong, P.M., Park, J., and Kane Breuer, C. Chapter forty—heart valves A2. In: Langer, R., and Vacanti, J., eds. Principles of Tissue Engineering, 3rd ed. Burlington: Academic Press, 2007. p. 585.
5. Kotecha, M., and Magin, R.L. MRI Assessment of Engineered Cartilage Tissue Growth. Magnetic Resonance Imaging in Tissue Engineering. Hoboken, NJ: John Wiley & Sons, Inc., 2017, p. 179.
6. Kotecha, M. Principles and Applications of Quantitative Parametric MRI in Tissue Engineering. Magnetic Resonance Imaging in Tissue Engineering. Hoboken, NJ: John Wiley & Sons, Inc., 2017, p. 21.
7. Amini, A.R., and Nukavarapu, S.P. Oxygen-tension controlled matrices for enhanced osteogenic cell survival and performance. Ann Biomed Eng **42,** 1261, 2014.
8. Mohyeldin, A., Garzon-Muvdi, T., and Quinones-Hinojosa, A. Oxygen in stem cell biology: a critical component of the stem cell niche. Cell Stem Cell **7,** 150, 2010.
9. Mathieu, J., Zhang, Z., Nelson, A., Lamba, D.A., Reh, T.A., Ware, C., and Ruohola-Baker, H. Hypoxia induces reentry of committed cells into pluripotency. Stem Cells **31,** 1737, 2013.
10. Simon, M.C., and Keith, B. The role of oxygen availability in embryonic development and stem cell function. Nat Rev Mol Cell Biol **9,** 285, 2008.
11. Barkai, U., Weir, G.C., Colton, C.K., Ludwig, B., Bornstein, S.R., Brendel, M.D., Neufeld, T., Bremer, C., Leon, A., Evron, Y., Yavriyants, K., Azarov, D., Zimermann, B., Maimon, S., Shabtay, N., Balyura, M., Rozenshtein, T., Vardi, P., Bloch, K., de Vos, P., and Rotem, A. Enhanced oxygen supply improves islet viability in a new bioartificial pancreas. Cell Transplant **22,** 1463, 2013.
12. Colton, C.K. Oxygen supply to encapsulated therapeutic cells. Adv Drug Deliv Rev **67–68,** 93, 2014.
13. Epel, B., Kotecha, M., and Halpern, H.J. In Vivo EPR Oxygen Imaging. Magnetic Resonance Imaging in Tissue Engineering. Hoboken, NJ: John Wiley & Sons, Inc., 2017, p. 129.
14. Brennan, M.D., Rexius-Hall, M.L., and Eddington, D.T. A 3D-printed oxygen control insert for a 24-well plate. PLoS One **10,** e0137631, 2015.
15. Brennan, M.D., Rexius-Hall, M.L., Elgass, L.J., and Eddington, D.T. Oxygen control with microfluidics. Lab Chip **14,** 4305, 2014.

16. Einstein, S.A., Weegman, B.P., Kitzmann, J.P., Papas, K.K., and Garwood, M. Noninvasive assessment of tissue-engineered graft viability by oxygen-17 magnetic resonance spectroscopy. Biotechnol Bioeng **114,** 1118, 2017.
17. Einstein, S.A., Weegman, B.P., Firpo, M.T., Papas, K.K., and Garwood, M. Development and validation of noninvasive magnetic resonance relaxometry for the in vivo assessment of tissue-engineered graft oxygenation. Tissue Eng Part C Methods **22,** 1009, 2016.
18. Epel, B., Redler, G., and Halpern, H.J. How in vivo EPR measures and images oxygen. Adv Exp Med Biol **812,** 113, 2014.
19. Redler, G., Epel, B., and Halpern, H.J. What we learn from in vivo EPR oxygen images. Adv Exp Med Biol **812,** 121, 2014.
20. Epel, B., Bowman, M.K., Mailer, C., and Halpern, H.J. Absolute oxygen R1e imaging in vivo with pulse electron paramagnetic resonance. Magn Reson Med **72,** 362, 2014.
21. Epel, B., Bowman, M.K., Mailer, C., and Halpern, H.J. Absolute oxygen R imaging in vivo with pulse electron paramagnetic resonance. Magn Reson Med **72,** 362, 2014.
22. Epel, B., and Halpern, H. Electron paramagnetic resonance oxygen imaging in vivo. Electron Paramagn Reson **23,** 180, 2013.
23. Epel, B., Sundramoorthy, S.V., Mailer, C., and Halpern, H.J. A versatile high speed 250 MHz pulse imager for biomedical applications. Concepts Magn Reson Part B Magn Reson Eng **33B,** 163, 2008.
24. Elas, M., Ahn, K.H., Parasca, A., Barth, E.D., Lee, D., Haney, C., and Halpern, H.J. Electron paramagnetic resonance oxygen images correlate spatially and quantitatively with oxylite oxygen measurements. Clin Cancer Res **12,** 4209, 2006.
25. Epel, B., Kotecha, M., and Halpern, H. In vivo preclinical cancer and tissue engineering applications of absolute oxygen imaging using pulse EPR. J Magn Reson **280,** 149, 2017.
26. Epel, B., Kotecha, M., and Halpern, H. In vivo EPR oxygen imaging: a case for tissue engineering. In: Kotecha, M., Magin, R., and Mao, J.J., eds. Magnetic Resonance Imaging in Tissue Engineering. Hoboken, NJ: Wiley, 2017, p. 129.
27. Amini, A.R., Adams, D.J., Laurencin, C.T., and Nukavarapu, S.P. Optimally porous and biomechanically compatible scaffolds for large-area bone regeneration. Tissue Eng Part A **18,** 1376, 2012.
28. Amini, A.R., Xu, T.O., Chidambaram, R.M., and Nukavarapu, S.P. Oxygen tension-controlled matrices with osteogenic and vasculogenic cells for vascularized bone regeneration in vivo. Tissue Eng Part A **22,** 610, 2016.
29. Majumdar, S., Pothirajan, P., Dorcemus, D., Nukavarapu, S., and Kotecha, M. High field sodium MRI assessment of stem cell chondrogenesis in a tissue-engineered matrix. Ann Biomed Eng **44,** 1120, 2016.
30. Dorcemus, D., George, E., Dealy, C., and Nukavarapu, S. Harnessing external cues: development and evaluation of an in vitro culture system for osteochondral tissue engineering. Tissue Eng Part A **23,** 719, 2017.
31. Ravindran, S., Kotecha, M., Huang, C.C., Ye, A., Pothirajan, P., Yin, Z., Magin, R., and George, A. Biological and MRI characterization of biomimetic ECM scaffolds for cartilage tissue regeneration. Biomaterials **71,** 58, 2015.
32. Ravindran, S., Gao, Q., Kotecha, M., Magin, R.L., Karol, S., Bedran-Russo, A., and George, A. Biomimetic extracellular matrix-incorporated scaffold induces osteogenic gene expression in human marrow stromal cells. Tissue Eng Part A **18,** 295, 2012.
33. Newby, D., Marks, L., and Lyall, F. Dissolved oxygen concentration in culture medium: assumptions and pitfalls. Placenta **26,** 353, 2005.

Address correspondence to:
Mrignayani Kotecha, PhD
O2M Technologies, LLC
2242 West Harrison Street
STE 201-18
Chicago, IL 60612

E-mail: mrignayani.kotecha@gmail.com

Boris Epel, PhD
Department of Radiation and Cellular Oncology
Center for EPR Imaging In Vivo Physiology
The University of Chicago
Chicago, IL 60637

E-mail: bepel@uchicago.edu

Received: April 29, 2017
Accepted: August 21, 2017
Online Publication Date: October 9, 2017